HEFAT2007
5th International Conference on Heat Transfer, Fluid Mechanics and Thermodynamics
Sun City, South Africa
Paper number: NA3

NUMERICAL PREDICTION OF DEVELOPING FLOW IN GAS PIPELINES

Nouri-Borujerdi, A.* and Ziaei-Rad, M.
*Author for correspondence
School of Mechanical Engineering, Sharif University of Technology
Azadi Avenue, Tehran, Iran
E-Mail: anouri@sharif.edu

ABSTRACT

In this paper the numerical modeling of the dynamic behavior of compressible gas flow is investigated in pipelines. The numerical simulation is performed by solving the coupled conservation form of the governing equations for two-dimensional, laminar, viscous, supersonic flow in developing region under different thermal boundary conditions. The numerical procedure is a finite-volume based finite-element method applied on unstructured grids. The convection terms are discretized by well-defined Roe Method and diffusion terms by a Galerkin finite element formulation. The temporal terms are evaluated based on an explicit fourth order Runge-Kutta scheme.

The results indicate that heating the gas flow leads to an increase in pressure loss. In the other words, cooling the gas flow leads to decrease the pressure drop or power consumption of booster pressure station. Furthermore, change in the gas viscosity has considerable effects on the flow quantities such as pressure loss and friction factor.

INTRODUCTION

The gas flow in pipelines is usually unsteady due to the occurrence of rapid and slow disturbances. The slow disturbances are associated with the compression and expansion of the gas in the pipeline due to pressure and mass flow fluctuations. They are caused by the cyclic variation in the gas demand. The Rapid disturbances are associated with wave effects caused by sharp closure of a shut off valve.

There have been many studies of compressible gas flow in pipelines in textbooks, articles and technical documents. Two limiting cases, adiabatic and isothermal, are often considered as thermal conditions. Adiabatic flow conditions assume flow through an insulated pipe. These conditions are usually valid for short pipelines since there is little heat transfer to or from the gas. Isothermal flow conditions assume flow through a pipe held at a uniform temperature; these conditions are commonly assumed when studying the flow of a gas in an uninsulated pipeline. Most natural gas pipelines are considered isothermal. Specially the analysis of flows and pressure drops in piping systems has been studied by many workers and is usually based upon the consideration of steady state conditions.

Many attempts have been done by researchers to reduce the pressure loss along the gas pipeline in order to reduce the costs of transportation. One of the main areas in pressure loss reduction techniques is lining the gas pipelines with smooth coatings to reduce the frictional pressure drop [1]. Another method is using chemicals [2], for example in cold weather and when the pipeline capacity needs to be increased in a period of time. New surfaces is another technique concern the making so special patterns on pipeline walls, in some cases to simulate natural surfaces, resulting in pressure loss reduction. Condensate systems are also used to find out whether the pressure loss reduction effects in natural gas pipelines, also apply when a liquid fraction is present. Experimental results on external flows [3] show that heating the gas can reduce the skin friction. Very significant drag reduction will be achieved if the beginning part of the model is heated.

Numerical simulation of unsteady internal compressible flows is the goal of many researchers during the years and several algorithms have been presented up to now. Mary et al. [4] proposed a second-order accurate algorithm for the simulation of unsteady viscous stratified compressible flows. The advantage of their method is its capability to deal with a broad range of subsonic Mach numbers, including nearly incompressible flows with a single modeling, based on the fully compressible Navier-Stokes equations. Solution of choked flow of low-density air through a narrow parallel plate channel with adiabatic walls was investigated by means of finite-difference numerical calculation by Shi et al. [5]. Toulopoulos and Ekaterinaris [6] investigated the application of second- and fourth-order accurate discontinuous Galerkin finite element method for the numerical solution of the Euler and the Navier-Stokes equations with triangular meshes. Xu et al. [7] presented

a finite volume formulation for large eddy simulation of turbulent pipe flows based on the compressible time dependent three-dimensional Navier–Stokes equations in Cartesian coordinates with non-Cartesian control volumes. Aydin [8] studied the effects of viscous dissipation on heat transfer in thermally developing laminar forced convection in a pipe with both constant heat flux and the constant wall temperature boundary conditions and obtained the distributions for the developing temperature and local Nusselt number in the entrance region and influence of Brinkman number (Br) and the thermal boundary conditions. Martineau and Berry [9] presented a new implicit continuous-fluid Eulerian scheme for simulating a wide range of transient and steady, inviscid and viscous compressible flows on unstructured finite elements which is developed as a predictor–corrector scheme by performing a fractional-step splitting of the semi-implicit temporal discretization of the governing equations into an explicit predictor phase and a semi-implicit pressure correction phase coupled by a pressure Poisson solution.

The above mentioned papers and other studies on unsteady compressible flow haven't focused significantly on the effect of thermal boundary conditions on pressure loss. In this paper a combined FV-FE unsteady procedure have been developed for the numerical solution of compressible viscous flow. The procedure is based on a general class of cell centered FV Roe Method for the discretization of inviscid parts together with the discretization of viscous terms by the FE method over a triangular grid. The effects of heating on pressure drop in unsteady pipe flow have been studied by details.

NOMENCLATURE

A	[m^2]	cell area, Jacobian matrix
b	[W/m^2]	Heat flux and work of frictional forces
c	[m^2,m/s]	triangle area, speed of sound
C_v	[J/Kg.K]	constant volume specific heat
D	[m^2]	pipe diameter
E	[J]	total internal energy
F	[$Kg/m^2 s$]	vector of inviscid flux terms
H	[$Kg/m.s^2$]	total enthalpy
k	[W/m.K]	Number of triangles, thermal conductivity
L	[m]	length of the pipe
N	[W/m^2]	vector of viscous flux terms
$\vec{n}$	[-]	unit normal vector
Pr	[-]	Prandtl number, $\mu C_p / k$
p	[N/m^2]	pressure
Q	[-]	vector of conservative variables
q	[W/m^2]	heat flux
R	[-]	matrix of eigenvectors
Re	[-]	Reynolds number, $\rho VD / \mu$
RHS	[-]	right hand side terms of governing equation
r	[m]	radial direction
S	[-]	source term
T	[K]	temperature
t	[s]	time
U	[-]	vector of primitive variables
$u_{r,z}$	[m/s]	velocity components
V	[m/s]	velocity vector
W	[-]	vector of characteristic variables
z	[m]	streamwise direction

Special characters

α	[-]	constant coefficient for Runge-Kutta method
Δ	[-]	difference
γ	[-]	specific heat ratio
μ	[$N.s/m^2$]	dynamic viscosity
ρ	[Kg/m^3]	density
τ	[N/m^2]	shear stress tensor
ϕ	[-]	shape function for F.E. formulation
Λ	[-]	matrix of eigenvalues
Ω	[-]	computational domain
Ψ	[-]	vector of auxiliary variables
∇	[-]	operator

Subscripts

c	pipe centerline
h	discretized computational domain
in	inflow
i, j, k	counter indices
L	lower cell index
n	normal to the control volume boundary
out	outflow
R	upper cell index
r, θ, z	associated with cylindrical direction
S	Sutherland law constant
t	tangential to the control volume boundary
w	wall
0	reference quantity

Superscripts

$n+1/n$	new/old quantity in iteration
$*$	dimensional variable
$\wedge$	Roe-average of a quantity

GOVERNING EQUATIONS

For gas flow with variable properties such as density and viscosity, the compressible Navier-Stokes equations are applicable even if a low-speed case is dealt with. First of all, the following variables are used to nondimensionalize the governing equations.

$$
\begin{aligned}
z^* &= z/D, & r^* &= r/D \\
u^* &= u/V_0, & \rho^* &= \rho/\rho_0 \\
t^* &= tV_0/D, & p^* &= p/\rho_0 V_0^2 \\
T^* &= C_v T/V_0^2, & \mathrm{Re}_0 &= \rho_0 V_0 D/\mu_0 \\
\mu^* &= \mu/(\mu_0 \mathrm{Re}_0), & k^* &= k/k_0 \\
q^* &= q/\rho_0 V_0^3, & e_t^* &= e_t/V_0^2
\end{aligned}
\qquad (1)
$$

where the superscript $'*'$ denotes the dimensional variables and the subscript '0' denotes values at a reference state. D, V_0, ρ_0 and μ_0 are the pipe diameter, inflow bulk velocity, density, temperature and viscosity, respectively at the reference state. After dropping the superscript '*', the conservative form of the nondimensionalized governing equations in the cylindrical coordinates system is as follows.

Conservation of mass

$$\frac{\partial \rho}{\partial t} + \frac{\partial(\rho u_z)}{\partial z} + \frac{1}{r}\frac{\partial(r\rho u_z)}{\partial r} = 0 \qquad (2)$$

Conservation of momentum

$$\frac{\partial(\rho u_z)}{\partial t}+\frac{\partial(\rho u_z^2+p)}{\partial z}+\frac{1}{r}\frac{\partial(r\rho u_r u_z)}{\partial r} = \frac{\partial \tau_{zz}}{\partial z}+\frac{1}{r}\frac{\partial(r\tau_{rz})}{\partial r} \quad (3a)$$

$$\frac{\partial(\rho u_r)}{\partial t}+\frac{\partial(\rho u_r u_z)}{\partial z}+\frac{1}{r}\frac{\partial\left[r(\rho u_z^2+p)\right]}{\partial r} = \frac{\partial \tau_{zr}}{\partial z}+\frac{1}{r}\frac{\partial(r\tau_{rr})}{\partial r}-\frac{\tau_{\theta\theta}}{r} \quad (3b)$$

Conservation of energy

$$\frac{\partial(\rho e_t)}{\partial t}+\frac{\partial\left[(\rho e_t+p)u_z\right]}{\partial z}+\frac{1}{r}\frac{\partial\left[r(\rho e_t+p)u_r\right]}{\partial r} = \frac{\partial b_z}{\partial z}+\frac{1}{r}\frac{\partial(rb_r)}{\partial r} \quad (4)$$

In the above equations, u_z, u_r are the axial and radial velocity components respectively and e_t is the total internal energy and is defined based on the perfect gas law as:

$$e_t=\frac{p}{\rho(\gamma-1)}+\frac{1}{2}\left(u_z^2+u_r^2\right) \quad (5)$$

Heat flux and surface work done by frictional forces terms in energy equation are defined as

$$b_z=k\frac{\partial T}{\partial z}+u_z\tau_{zz}+u_r\tau_{zr}$$
$$b_r=k\frac{\partial T}{\partial r}+u_z\tau_{zr}+u_r\tau_{rr} \quad (6)$$

and viscous stress terms for the tensor components are:

$$\tau_{zz}=\mu\left[2\frac{\partial u_z}{\partial z}-\frac{2}{3}\left(\nabla.\vec{V}\right)\right] \quad (7a)$$

$$\tau_{zr}=\mu\left[\frac{\partial u_z}{\partial r}+\frac{\partial u_r}{\partial z}\right] \quad (7b)$$

$$\tau_{rr}=\mu\left[2\frac{\partial u_r}{\partial z}-\frac{2}{3}\left(\nabla.\vec{V}\right)\right] \quad (7c)$$

$$\tau_{\theta\theta}=\mu\left[2\frac{u_r}{r}-\frac{2}{3}\left(\nabla.\vec{V}\right)\right] \quad (7d)$$

where

$$\nabla.\vec{V}=\frac{\partial u_z}{\partial z}+\frac{1}{r}\frac{\partial}{\partial r}(r\,u_r) \quad (8)$$

The temperature-dependent viscosity based on the Sutherland law's is:

$$\mu=\mu_0\left(\frac{T}{T_0}\right)^{3/2}\left(\frac{T_0+T_S}{T+T_S}\right) \quad (9)$$

where T_S is the Sutherland constant temperature.

Looking at the conservative form of the governing equations, we note that they all have the same generic form, given by

$$\frac{\partial Q}{\partial t}+\nabla.F(Q)=\nabla.N(Q)+S(Q) \quad (10)$$

$Q, F_z(Q)$, $N(Q)$ and $S(Q)$ are the conservative variables, inviscid flux , viscous flux and source vector respectively.

$$Q=\left[\rho \quad \rho u_z \quad \rho u_r \quad \rho e_t\right]^T \quad (11)$$

The inviscid flux vector $F(Q)$ includes components $F_z(Q)$ and $F_r(Q)$ with the following expressions

$$F_z(Q)=\left[\rho u_z \quad \rho u_z^2+p \quad \rho u_z u_r \quad (\rho e_t+p)u_z\right]^T$$
$$F_r(Q)=\left[\rho u_r \quad \rho u_z u_r \quad \rho u_r^2+p \quad (\rho e_t+p)u_r\right]^T \quad (12)$$

The viscous flux vector $N(Q)$ also includes $N_z(Q)$ and $N_r(Q)$ with the following forms.

$$N_z(Q)=\left[0 \quad \tau_{zz} \quad \tau_{zr} \quad b_z\right]^T$$
$$N_r(Q)=\left[0 \quad \tau_{rz} \quad \tau_{rr} \quad b_r\right]^T \quad (13)$$

The source vector for axisymmetric flow is written as

$$S(Q)=\left[0 \quad 0 \quad -\tau_{\theta\theta}/r \quad 0\right]^T \quad (14)$$

Having solved the set of governing equations, the distribution of the thermodynamic variables of gas flow in the pipeline can be found.

NUMERICAL TECHNIQUE

The Navier-Stokes equations for the compressible viscous flow are solved by a finite volume-Galerkin upwind technique using the Roe [10] Riemann Solver for the convective part and standard Galerkin technique for the viscous terms.

If $\Omega=K_jC_j$ be a discretization by triangles of computational domain Ω where C is the triangle area and K is the number of triangles and $\Omega=K_iA_i$ be its partition in cells where A_i is cell areas, thus we suppose that F varies linearly on each triangle.

We move the additional terms of the cylindrical operator of equation (10) compare to the Cartesian operator to the right

hand side of the equation as source terms to use the two dimensional Cartesian coordinate system.

Figure 1 shows the triangulation of computational domain and computational nodes. The variables will be computed on nodes denote by subscript h. If they are the vertices of triangle elements, these nodes are related to finite element grid. Otherwise, they are related to the control volume in the center of the hexagonal finite volume grid.

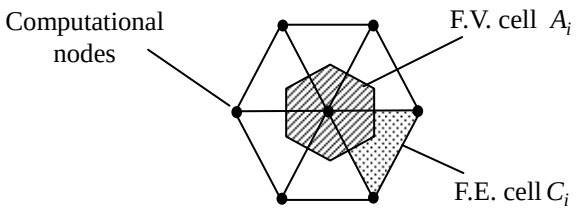

Figure 1 Triangulation of computational domain Ω

The weak finite element formulation of governing equation (10) without the source term can be written as

$$\int_{\Omega} \frac{\partial Q_h}{\partial t} \phi_h dA + \int_{\Omega} \nabla.\left(F_h - N_h\right)\phi_h dA = 0 \qquad (15)$$

where ϕ is the shape function which is set equal to one in the finite volume calculations. In the finite element, it is computed from the geometry and is used to compute the derivations. For example the derivation of a quantity e with respect to coordinate z is as: $\partial e/\partial z = e_1 \partial\phi_1/\partial z + e_2 \partial\phi_2/\partial z + e_3 \partial\phi_3/\partial z$

Indices 1, 2, and 3 are related to three vertices of the triangle and ϕ_1, ϕ_2 and ϕ_3 are their shape functions.

Integrating the viscous term *N* using part by part method and remaining the convective term *F* in its original form with shape function one, results in:

$$\int_{\Omega} \frac{\partial Q_h}{\partial t} \phi_h dA + \int_{\Omega} \nabla.F_h dA + \int_{\Omega} N_h \nabla\phi_h dA - \int_{\partial\Omega} N_h.n\phi_h dC = 0 \qquad (16)$$

The first term is the time-dependent one. The second and third terms respectively show the variation of inviscid and viscous parts on the cell. The fourth term is associated with boundary treatment.

Using explicit time integration and introducing divergence theorem for convective part, the final formulation is obtained as follows.

$$\left|A_i\right| \frac{Q^{n+1} - Q^n}{\Delta t} + \int_{\partial C_i} F_d.n\, dC = -\int_{\Omega_h} N_h \nabla\phi_h dA + \int_{\partial\Omega} N_h.n\,\phi_h dC \qquad (17)$$

The superscripts *n* and *n+1* denotes the old and new time steps respectively. A centered scheme is used to compute the viscous part on each cell. The source term is computed explicitly.

The second term on the right-hand side of equation (17) is related to boundary condition which is set to be zero herein and the boundary condition will be applied in finite volume formulation of convective terms. The convection term on the left hand side is evaluated by finite volume Roe method [10] on control volume surfaces which are the sides of hexagonal shape. In this way the flux vector across these planes is computed from

$$F = \frac{1}{2}\left(F_L + F_R\right) - \frac{1}{2} R\left|\Lambda\right| \Delta Q \qquad (18)$$

where R is the eigenvector matrix of the Jacobian matrix $A = \partial F/\partial Q$, where:

$$A = \begin{bmatrix} 0 & n_z & n_r & 0 \\ -u_z u_n + \frac{\gamma-1}{2}V^2 n_z & (2-\gamma)u_z n_z + u_n & u_z n_r + (1-\gamma)u_r n_z & (\gamma-1)n_z \\ -u_r u_n + \frac{\gamma-1}{2}V^2 n_r & u_r n_z + (1-\gamma)u_z n_r & (2-\gamma)u_r n_r + u_n & (\gamma-1)n_r \\ -u_n\left(H - \frac{\gamma-1}{2}V^2\right) & H n_z + (1-\gamma)u_z u_n & H n_r + (1-\gamma)u_r u_n & \gamma u_n \end{bmatrix} \qquad (19)$$

$$R = \begin{bmatrix} 1 & 0 & 1 & 1 \\ \hat{u} - \hat{c}.n_x & -\hat{u}_t n_y & \hat{u} & \hat{u} + \hat{c}.n_x \\ \hat{v} - \hat{c}.n_y & \hat{u}_t n_x & \hat{v} & \hat{v} + \hat{c}.n_y \\ \hat{H} - \hat{u}_n \hat{c} & \hat{u}_t^2 & \frac{1}{2}\hat{V}^2 & \hat{H} + \hat{u}_n \hat{c} \end{bmatrix} \qquad (20)$$

Normal and tangential velocity components u_n and u_t are defined, respectively as:

$$\hat{u}_n = \hat{u}.n_x + \hat{v}.n_y$$
$$\hat{u}_t = \hat{v}.n_x - \hat{u}.n_y$$

F_R and F_L are the flux vectors computed from the right and left states of Q_R and Q_L and $\Delta Q = Q_R - Q_L$. $\left|\Lambda\right|$ is a diagonal matrix of eignvalues of Jacobian matrix which includes three characteristics with speeds $\hat{u}_n - \hat{c}$, $\hat{u}_n$, $\hat{u}_n$, $\hat{u}_n + \hat{c}$, where $\hat{c}$ is the sound speed. The hats refer to Roe-average of a quantity computed for $\hat{u}_r$, $\hat{u}_z$ and $\hat{H}$ by weighting with $\sqrt{\rho}$, as follow

$$\hat{u} = \frac{u_L\sqrt{\rho_L} + u_R\sqrt{\rho_R}}{\sqrt{\rho_L} + \sqrt{\rho_R}} \qquad (21)$$

The other quantities with hats in eigenvector arrays are not averaged independently, but are the basic Roe-averaged quantities by their normal functional relation. More details of Roe method can be found in [10].

Finally the governing equation (10) can be re-write as

$$\frac{\partial Q}{\partial t} = RHS(Q) \tag{22}$$

where $RHS(Q)$ contains convective, viscous and source terms. The time integration procedure has been done explicitly using a fourth order Runge-Kutta scheme as follow

$$\begin{aligned} &Q_0 = Q^n \\ &Q_i = Q_i + \alpha_i \frac{\Delta t}{|A|} RHS(Q_{i-1}) \qquad for\ i = 1,...,4 \\ &Q^{n+1} = Q_4 \end{aligned} \tag{23}$$

where $RHS(Q_{i-1})$ consists of convective, diffusive and source terms in the previous time step. The optimum choice for α_i is as follows, [11].

$$\alpha_1 = 0.11, \quad \alpha_2 = 0.2766, \quad \alpha_3 = 0.5, \quad \alpha_4 = 1.0 \tag{24}$$

This scheme enables us to investigate the treatment of time dependent pipe flow.

BOUNDARY CONDITIONS

The governing equations require the specification of the boundary conditions at the wall, inlet and outlet due to the elliptic nature of the equations. The classical boundary condition for velocity on solid walls is no-slip condition, namely $\vec{V} = 0$. On the symmetry line of the pipe, symmetry boundary condition ($\vec{V}.\vec{n} = 0$) is also necessary.

At the pipe inlet the flow is subsonic and two primitive variables should be specified there, where for subsonic outflow only one variable is required. Inflow and outflow boundaries are treated by a new characteristics technique. Along these boundaries the fluxes are splitted in positive and negative parts following the sign of the eignvalues for the Jacobian $A = \partial F / \partial Q$ of the convective operator F, [12]. The system of equations can be written in the characteristic form as

$$\frac{\partial W}{\partial t} + \Lambda \nabla . W = \tilde{S} \tag{25}$$

with $\partial W = L \partial Q$ and $\tilde{S} = L S$. We select well-posed boundary conditions by prescribing the characteristic variables whose convection velocity direction is towards the interior of the domain at the boundary. In this way, the number of boundary conditions is a function of the signs of the eigenvalues of Λ, [13].

The boundary conditions are simpler to implement if we consider the set of primitive variables

$$U = \begin{pmatrix} \rho & u_z & u_r & p \end{pmatrix}^T \tag{26}$$

which are related to the set of conservative variables by

$$\frac{\partial Q}{\partial U} = \begin{bmatrix} 1 & 0 & 0 & 0 \\ u_z & \rho & 0 & 0 \\ u_r & 0 & \rho & 0 \\ \frac{1}{2}V^2 & \rho u_z & \rho u_r & \frac{1}{\gamma - 1} \end{bmatrix} \tag{27}$$

The characteristic variables, written as functions of the primitive variables, take the form

$$\partial W = \begin{bmatrix} \partial W_1 \\ \partial W_2 \\ \partial W_3 \\ \partial W_4 \end{bmatrix} = \frac{\partial W}{\partial U} \partial U = \begin{bmatrix} \partial \rho + c^{-2} \partial p \\ \partial \rho - c^{-2} \partial p \\ \partial u_n + (\rho c)^{-1} \partial p \\ \partial u_n - (\rho c)^{-1} \partial p \end{bmatrix} \tag{28}$$

where the Jacobian matrix of the transformation is given by

$$\frac{\partial W}{\partial U} = \begin{bmatrix} I_1 \\ I_2 \\ I_3 \\ I_4 \end{bmatrix} = \begin{bmatrix} 1 & 0 & 0 & c^{-2} \\ 1 & 0 & 0 & -c^{-2} \\ 0 & n_z & n_r & (\rho c)^{-1} \\ 0 & n_z & n_r & -(\rho c)^{-1} \end{bmatrix} \tag{29}$$

n_z, n_r are unit vectors in axial and radial directions, respectively. The inlet boundary conditions for steady-state consist of imposing the gas density ρ, axial velocity u_z, and radial velocity u_r, which is set to be zero at the inlet. The fourth equation is determined from the characteristic property that is convected outwards with respect to the domain, ∂W_4, resulting in an inlet state given by

$$Q_{in}(t) = Q_{in}(x^+_{1/2}, t) + \frac{\partial Q}{\partial U} \frac{\partial U}{\partial \Psi}\bigg|_{in} \Delta \Psi_{in} \tag{30}$$

with

$$\partial \Psi_{in} = \begin{pmatrix} \partial \rho & \partial u_z & \partial u_r & \partial W_4 \end{pmatrix} \tag{31}$$

$$\frac{\partial \Psi}{\partial U}\bigg|_{in} = \left(\frac{\partial U}{\partial \Psi}\bigg|_{in} \right)^{-1} = \begin{bmatrix} \frac{\partial \rho}{\partial \rho} & \frac{\partial \rho}{\partial u_z} & \frac{\partial \rho}{\partial u_r} & \frac{\partial \rho}{\partial p} \\ \frac{\partial u_z}{\partial \rho} & \frac{\partial u_z}{\partial u_z} & \frac{\partial u_z}{\partial u_r} & \frac{\partial u_z}{\partial p} \\ \frac{\partial u_r}{\partial \rho} & \frac{\partial u_r}{\partial u_z} & \frac{\partial u_r}{\partial u_r} & \frac{\partial u_r}{\partial p} \\ 0 & n_x & n_y & -(\rho c)^{-1} \end{bmatrix} \tag{32}$$

and

$$\Delta\Psi_{in} = \begin{bmatrix} \rho_{in} - \rho\left(x^{+}_{1/2}, t\right) \\ u_{z,in} - u_z\left(x^{+}_{1/2}, t\right) \\ u_{r,in} - u_r\left(x^{+}_{1/2}, t\right) \\ 0 \end{bmatrix} \quad (33)$$

Subscript *1/2* denotes the domain interior point at the inflow. The forth row of the Jacobian matrix in equation (32) is taken from the forth row of the matrix in equation (29). The derivatives that appear in the Jacobian matrix in equation (32) are evaluated analytically.

At outlet boundary, we set the pressure, p, which must be imposed at subsonic outflow. The other three boundary conditions to be imposed are the characteristic variables that are convected towards the exterior of the domain, ∂W_1, ∂W_2 and ∂W_3, from which we obtain

$$Q_s(t) = Q\left(x^{-}_{N+1/2}, t\right) + \left.\frac{\partial Q}{\partial \Psi}\right|_{out} \Delta\Psi_{out} \quad (34)$$

with

$$\partial\Psi_{out} = \left[\partial W_1 \quad \partial W_2 \quad \partial W_3 \quad \partial p\right]^T \quad (35)$$

$$\Delta\Psi_{out} = \left[0 \quad 0 \quad 0 \quad p_{out} - p_{x^{-}_{N+1/2,t}}\right]^T \quad (36)$$

subscript (*N+1/2*) denotes the domain interior point at the outflow. The Jacobian matrix, ($\partial Q / \partial \Psi_{out}$), is determined in an analogous way to the previous case.

For thermal boundary conditions, two separate cases are considered.

Constant Wall Heat Flux: Under this condition, the heat addition to the gas flow from the pipe wall is subjected to a uniform heat flux and N_h is replaced by q'' in the fourth term of the conservative variables vector in equation (16).

Constant wall temperature: In this case, the pipe wall is at a constant temperature. Since the velocity vector is also zero on the wall, the forth conservative variable, e_t, at the wall will be $e_t = C_v T_w$, where T_w is wall temperature.

INITIAL CONDITIONS

The initial conditions for transient flow are given by the steady-state flow solution with prescribed inlet and outlet conditions. This steady-state solution is obtained by running the solver that implements the above formulation, starting from an arbitrary physically consistent initial condition and imposing the steady-state boundary conditions, until the desired degree of convergence is achieved. The initial condition selected in this paper is a steady state solution of gas flow with adiabatic pipe wall.

RESULTS AND DISCUSSION

The computational domain for the gas flow in the entrance region of a pipe is depicted in figure 2. Because of the pipe symmetry, half section of the pipe is selected as a computational domain. An unstructured triangular grid in the z and r directions is employed. In order to get better resolution on boundary layer, inflow and outflow, the meshes are fined in these positions. Several mesh sizes were tested to insure that the solution is not mesh dependent and finally a mesh contains 2121 nodes and 4000 elements were used for a pipe of 25m length and 1m diameter. The computations are done for methane which its properties are summarized in table 1.

Table 1 Properties of Methane at 15 ^{o}C

Parameter	Value	Unit
Molar weight	16.01	gr/mole
specific Heat	2260	J/Kg.K
specific heat ratio	1.299	-
Prandtl Number	0.71	-
heat conductivity	0.035	W/m.K
viscosity	1.1083×10^{-5}	N.s/m^2

If the Prandtl number is assumed constant, thermal conductivity can be calculated from the equation:

$$k = \frac{\mu C_p}{Pr} \quad (37)$$

Before proceeding to computation, the reference quantities are designated by index '0' in the governing equations as: $\mathrm{Re}_0 = 1000$, $T_0 = 300K$, $M_0 = 0.2$ and $\mu_0 = 1.1\times10^{-5}\, N.s/m^2$

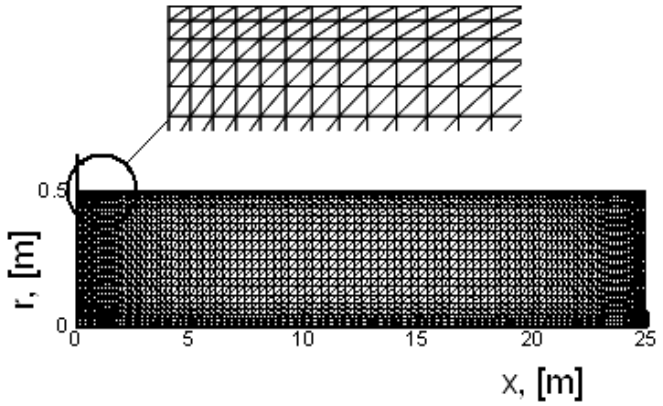

Figure 1 Schematic of computation domain of the pipe

Figure 3 depicts the development of velocity profiles in the gas pipeline for different wall heat fluxes. Because the momentum and energy equations are coupled in compressible flow, the velocity profile gets larger by increasing the heat flux on the wall. This means that the heating causes the velocity profile becomes more uniform across the pipe.

Figure 4 illustrates the time-dependent inlet pressure and temperature at different heat fluxes. The pressure and temperature profiles are the same. In this case it is assumed that the gas flow is suddenly subjected to a constant wall heat flux.

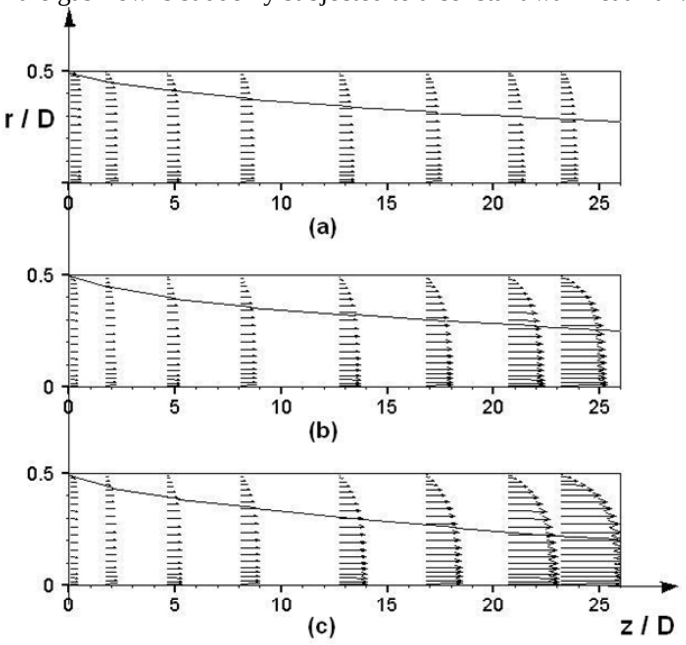

Figure 3 Development of gas velocity profile along the pipe for (a) q = 0, (b) q = 177.8 J/Kg, (c) q = 444.7 J/Kg

The results show that the required time to reaches a steady state depends on the heat flux. In the case of lower heating, more time is needed to reach a steady state. On the other hand, the peak values of pressure and temperature increase by increasing heat flux.

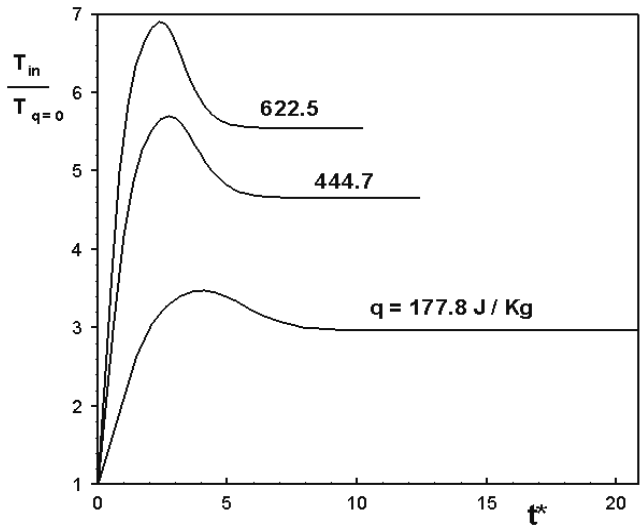

Figure 4 Inlet gas temperature profile for different heat fluxes

Figure 5 shows the variation of friction factor along the pipe for different heat fluxes on the pipe wall. The results are obtained for a constant pressure difference between the inlet and outlet of the pipe, $\Delta p^* = 4$. The friction coefficient increases with increase in heat flux. Therefore, it causes either more pressure drop or less mass flow rate occurs in the pipe.

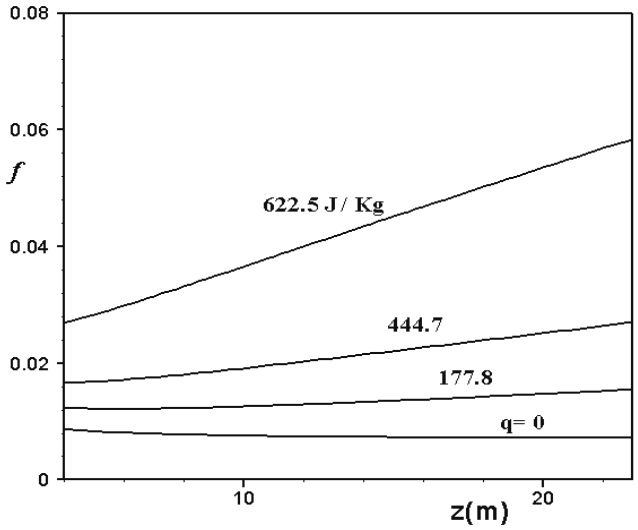

Figure 5 Average friction factor along the pipe for $\Delta p^* = 4$

Figure 6 indicates the variation of mass flow rate with the pressure ratio under different thermal conditions. In this graph, it is clear that heating will reduce the mass rate from the pipe for a specified pressure ratio. Therefore in order to increase the rate of gas from pipeline between two stations, one should reduce the rate of heat transfer from the pipe wall.

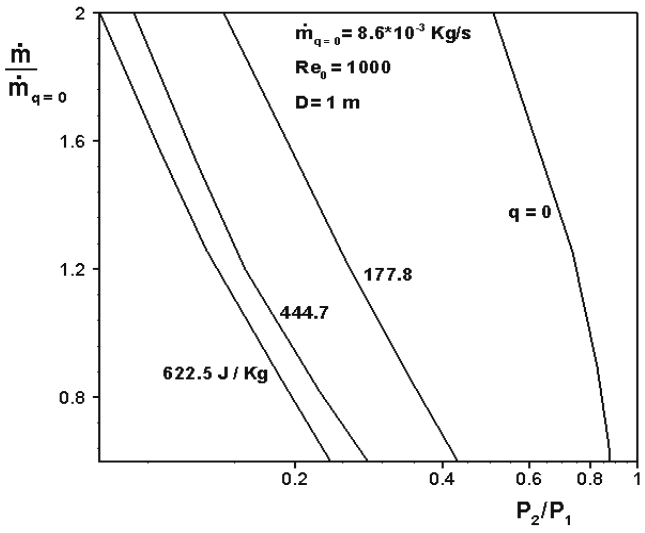

Figure 6 Inflow mass flow rate for different heat fluxes

Figure 7 shows an average gas temperature against the length of the pipe. The temperature is difference with heating of the pipe wall. Also the corresponding pressure drop for each case was shown on the figure and the enhancement of pressure loss with heating is obvious in this results.

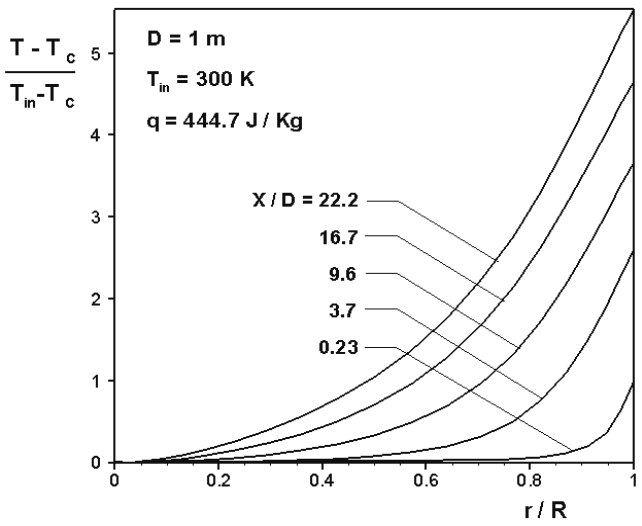

Figure 7 radial temperature profiles at different locations along the pipe

Effect of heating on mass flow rate for two various pressure losses is depicted in figure 8. A considerable result in this figure is that the pressure loss will be increased with heating, for a specified mass flow rate. However, since the Reynolds number in transportation gas pipelines is actually very high, the results of low Reynolds number are more reliable in this solution and for high Reynolds numbers, a suitable turbulence modeling in necessary.

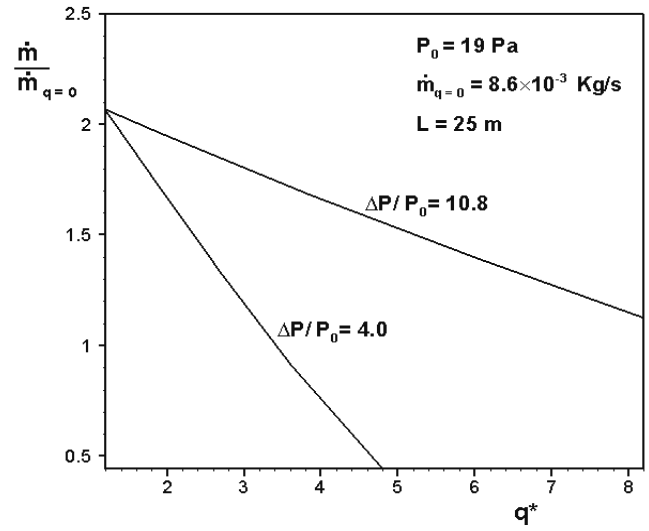

Figure 8 Inflow mass flow rate for different pressure losses

CONCLUDING REMARKS

Two dimensional compressible flow of natural gas transmission in pipelines with friction and heat addition are studied numerically. The results indicate that heating the gas flow leads to an increase in pressure loss. In the other words, in order to decrease the pressure loss, one should cool the gas. Furthermore, the results show that the change in the gas viscosity has considerable effects on the flow quantities such as pressure loss and variation of friction factor.

REFERENCES

[1] Zamorano R., Internal coating total gas transport cost reduction study, *Pipeline and Gas Journal*, October 2002.

[2] Sedahmed G.H., Abdo M.S.E., Amer M.A., El-Latif G.A., Effect of drag reducing polymers on the rate of mass transfer controlled corrosion in pipelines under developing turbulent flow, *Journal of Int. Comm. Heat Mass Transfer*, Vol.26, No.4, 1999, pp. 531-538

[3] Kramer B.R., Brooke C., Smith, J.P., Drag reduction experiments using boundary layer heating, *AIAA-99-0134*, 1999

[4] Mary I., Sagaut P., Deville M., An algorithm for low Mach number unsteady flows, *Computers & Fluids* 29, 2000, pp. 119-147

[5] Shi W., Miyamoto M., Katoh Y., Kurima J., Choked flow of low density gas in a narrow parallel plate channel with adiabatic walls, *Int. J. of Heat and Mass Transfer* 44, 2001, pp. 2555-2565

[6] Toulopoulos I., Ekaterinaris J. A., discontinuous Galerkin discretizations for viscous compressible flows, *5th GRACM International Congress on Computational Mechanics*, Limassol, 29 June – 1 July, 2005

[7] Xu X., Lee J.S., Pletcher R.H., A compressible finite volume formulation for large eddy simulation of turbulent pipe flows at low Mach number in Cartesian coordinates, *Journal of Computational Physics* 203, 2005, pp. 22–48

[8] Aydin O., Effects of viscous dissipation on the heat transfer in a forced pipe flow. Part 2: Thermally developing flow, *Energy Conversion and Management* 46, 2005, pp. 3091–3102

[9] Martineau R.C., Berry R.A., The pressure-corrected ICE finite element method for compressible flows on unstructured meshes, *Journal of Computational Physics 198*, 2004, pp. 659–685

[10] Roe P.L., Characteristic-based schemes for the Euler equations, *Journal of Ann. Rev. Fluid Mech.* 18, 1986, pp. 337-365

[11] Lallemand M.H., Schemas decentres multigrilles pour la resolution des equations D'Euler en elements finis, *Thesis, Univ. of Province-Saint Charles*, 1988

[12] Steger J., Warming R.F., Flux vector splitting for the inviscid gas dynamic with applications to finite-difference methods, *Journal of Computational Physics* 40, 1983, pp. 263-293

[13] Gato L.M.C., Henriques J.C.C., Dynamic behaviour of high-pressure natural-gas flow in pipelines, *International Journal of Heat and Fluid Flow* 26, 2005, pp. 817–825